Slow Electrons Generated by Intense High-Frequency Laser Pulses

Koudai Toyota,[1] Oleg I. Tolstikhin,[2] Toru Morishita,[1,3] and Shinichi Watanabe[1]

[1]*Department of Applied Physics and Chemistry, University of Electro-Communications, 1-5-1, Chofu-ga-oka, Chofu-shi, Tokyo, Japan*
[2]*Russian Research Center "Kurchatov Institute," Kurchatov Square 1, Moscow 123182, Russia*
[3]*PRESTO, Japan Science and Technology Agency, Kawaguchi, Saitama 332-0012, Japan*

(Received 16 July 2009; published 6 October 2009)

A very slow electron is shown to emerge when an intense high-frequency laser pulse is applied to a hydrogen negative ion. This counterintuitive effect cannot be accounted for by multiphoton or tunneling ionization mechanisms. We explore the effect and show that in the high-frequency regime the atomic electron is promoted to the continuum via a nonadiabatic transition caused by slow deformation of the dressed potential that follows a variation of the envelope of the laser pulse. This is a general mechanism, and a slow electron peak should always appear in the photoelectron spectrum when an atom is irradiated by a high-frequency pulse of finite length.

DOI: 10.1103/PhysRevLett.103.153003 PACS numbers: 32.80.Fb, 31.15.−p, 31.70.Hq, 32.80.Gc

The latest free electron laser technologies generate the coherent light sources in x-ray range. The wavelength, duration, and intensity of the pulses reach tens of nanometers, tens of femtoseconds, and 10^{12}–10^{16} W/cm^2, respectively [1–3]. This has extended the research area from the infrared to the high-frequency (HF) regime. The ionization dynamics in the two regimes is governed by quite distinct aspects. While the former has been more actively studied in recent years, interest in the latter is expected to grow in the nearest future. One well-established phenomenon in the HF regime is the atomic stabilization—a decrease of the ionization rate as a function of the laser intensity at sufficiently high intensities [4,5]. The study of this phenomenon proves that the Kramers-Henneberger (KH) frame [6,7] (in which the interaction with the laser field is transformed into a quiver motion of the atomic potential) and the high-frequency Floquet theory (HFFT) [8] (in which the quiver motion is averaged in time and the atomic stabilization is explained by the formation of a stationary state supported by a "dressed" potential) provide an adequate theoretical framework for the analysis of the HF regime. However, real pulses, even containing many optical cycles, have finite length. This circumstance may lead to surprising effects that are not accounted for by the HFFT. Recently, we proposed an adiabatic version of the HFFT [9,10] which enables one to take slow variations of the pulse envelope into account. This approach provides a powerful tool to understand the dynamics and interpret the photoelectron spectra in the HF regime. Using this approach, in this Letter we address some salient features of the physics in the HF regime. We present and explore an especially counterintuitive effect of generation of slow electrons by intense HF laser pulses. This effect is explained by an ionization mechanism which, as far as we know, has not been investigated previously.

We consider a negative ion H^- interacting with a laser pulse. The time-dependent Schrödinger equation (TDSE) in the single-active-electron approximation in the KH frame reads (atomic units are used throughout)

$$i\frac{\partial\psi(\mathbf{r},t)}{\partial t}=\left[-\frac{1}{2}\Delta+V(|\mathbf{r}+\boldsymbol{\alpha}(t)|)\right]\psi(\mathbf{r},t), \quad (1)$$

where $V(r)$ is the atomic potential and $\boldsymbol{\alpha}(t)$ is the classical trajectory of an electron in the laser field. The ion H^- is modeled by a Gaussian potential $V(r)=-V_0\exp(-r^2/r_0^2)$ which supports only one bound state with the correct energy $E_0=-0.027\,751\,0$ [10,11]. The electric field is represented by $\mathbf{F}(-T/2\le t\le T/2)=Ff(t/T)\times(\varepsilon\sin\omega t,0,\cos\omega t)$, where T is the pulse length. The envelope $f(\tau)$ is a bell-shaped function satisfying $f(-\tau)=f(\tau)$, $f(\pm1/2)=0$, and $\max f(\tau)=f(0)=1$. We choose it in such a way that $\dot{\boldsymbol{\alpha}}(\pm T/2)=\boldsymbol{\alpha}(\pm T/2)=\mathbf{0}$, so the photoelectron spectra in the KH and laboratory frames coincide [10]. We shall consider pulses with linear ($\varepsilon=0$) and circular ($\varepsilon=1$) polarizations. The maximum electron's excursion amplitude for such pulses is $\alpha_0=\max|\boldsymbol{\alpha}(t)|=F/\omega^2$. The main advantage of the KH frame for solving the TDSE [12], especially in the HF regime, is that the potential in Eq. (1) is localized in a finite region of the size $a\sim r_0+\alpha_0$. There is no electric field outside this region, so applying the outgoing-wave boundary conditions at its border one should be able to extract observables with minimum computational labor. Recently, one of us has developed a method which enables one to exactly incorporate the outgoing-wave boundary conditions [11,13,14]. The method is based on the expansion of the solution to the TDSE in terms of the Siegert states; it generalizes earlier applications of Siegert states for time propagation of wave packets [15–17] to nonstationary systems. The first applications of this method to the laser-atom interaction problem [9–11] have demonstrated its ability to produce very accurate highly resolved photoelectron spectra. Figure 1 shows typical spectra for H^- in the HF regime produced by pulses with $F=0.3$, $\omega=\pi/10$, and $T=2400$. The most prominent feature in such spectra is a series of above-threshold ionization

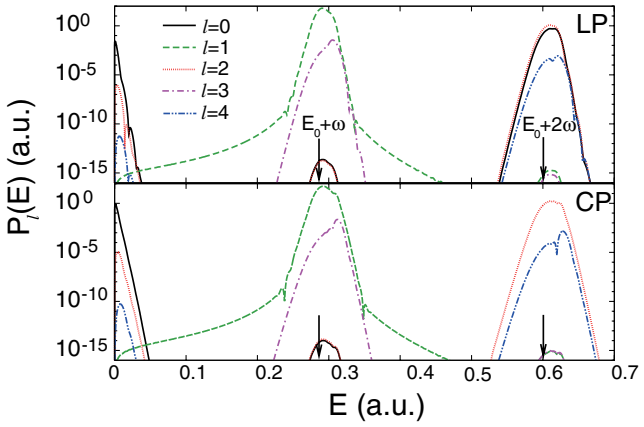

FIG. 1 (color online). Typical partial-wave photoelectron spectra for H^- produced by high-frequency pulses with linear (LP) and circular (CP) polarizations. The laser parameters are $F = 0.3$ ($I = 3.1 \times 10^{15}$ W/cm^2), $\omega = \pi/10 = 8.55$ eV, and $T = 2400 = 57.6$ fs, so the pulse contains 120 optical cycles and $\alpha_0 = 3.04$. In both cases, the total ionization probability is close to 99%. The arrows indicate the n-photon absorption energies $E_0 + n\omega$ for $n = 1$ and 2.

(ATI) peaks located at the n-photon absorption energies $E_0 + n\omega$ [18]. Even though the physics associated with ATI peaks is generally well understood [19], new features of ATI spectra continue to be uncovered.

In Refs. [9–11], we found and analyzed an oscillating substructure of ATI peaks in the atomic stabilization regime resulting from the interference of electrons ionized in the rising and falling parts of the pulse. Here we focus on another novel and general feature of the same spectra. One can notice an additional peak located at small photoelectron energies in Fig. 1. Let us call it the slow electron peak (SEP). The SEP exists for any polarization of the pulse. Similar SEPs can be found in spectra reported in [10,11]. Our calculations show that the SEP appears under the following conditions establishing a relation between three time scales in the problem:

$$\omega \gg |E_0|, \qquad \omega T \gg 1, \qquad |E_0| T \gg 1. \tag{2}$$

Trying to understand the origin of the SEP, first of all one has to rule out the channel closing mechanism. Indeed, in the HF regime the ponderomotive shifts of the bound state and ionization threshold are almost equal. Another possibility is multiphoton ionization followed by emission of the same number of photons. Because of a finite spectral width of the pulse, this process may produce slow electrons. However, it cannot explain the calculated dependencies of the SEP on the pulse parameters, at least not in any finite order. We mention tunneling, but only in order to exclude this mechanism also, since it has nothing to do with the properties of the HF regime. Known ionization mechanisms thus fail to account for the appearance of the SEP. In this Letter we propose a possible solution for this situation.

A natural framework to treat the regime defined by the first condition in (2) is the high-frequency Floquet theory [8]. In the monochromatic case, the potential in Eq. (1) can be expanded into the Fourier series,

$$V(|\mathbf{r} + \boldsymbol{\alpha}(t)|) = \sum_{n=-\infty}^{\infty} V_n(\mathbf{r}; \alpha_0) e^{in\omega t}. \tag{3}$$

In the lowest order of the HFFT, the electron is in a stationary state supported by the time-averaged or "dressed" potential $V_0(\mathbf{r}; \alpha_0)$. In the next order, its interaction with the other terms in Eq. (3), which represent multiphoton decay channels, is taken into account. Note that the dressed potential $V_0(\mathbf{r}; \alpha_0)$ depends on the excursion amplitude α_0 (as well as on the polarization of the laser field); it coincides with the original atomic potential $V(r)$ for $\alpha_0 = 0$, but may considerably differ from it for large values of α_0. In our case, the pulse is not monochromatic, but its envelope varies slowly. The second condition in (2) ensures that the problem can be treated using the adiabatic version of the HFFT [9,10]. This approach is implemented by substituting $\alpha_0 \to \alpha(t) = \alpha_0 f(t/T)$ into the right-hand side of Eq. (3). Neglecting all multiphoton processes, we thus arrive at the equation

$$i \frac{\partial \psi_0(\mathbf{r}, t)}{\partial t} = \left[-\frac{1}{2}\Delta + V_0(\mathbf{r}; \alpha(t)) \right] \psi_0(\mathbf{r}, t). \tag{4}$$

In contrast to Eq. (1), the Hamiltonian in Eq. (4) depends on time only via a slow time dependence of the envelope of the pulse; rapid oscillations of $\boldsymbol{\alpha}(t)$ at the laser frequency are averaged out by switching to the dressed potential. We shall call Eq. (4) the time-averaged TDSE.

Equation (4) does not account for multiphoton processes, but we expect that it correctly describes the physics associated with the SEP. To confirm this, we compare spectra obtained by solving Eqs. (1) and (4). The step from Eq. (1) to Eq. (4) is justified by the first two conditions in (2), so these conditions must be satisfied. We consider pulses of the same length $T = 2400$ as in Fig. 1. The spectra obtained from the full TDSE (1) depend on the field amplitude F and frequency ω separately, while those obtained from the time-averaged TDSE (4) depend only on their combination given by α_0. We solve Eqs. (1) for pulses with $F = n^2 F_0$ and $\omega = n\omega_0$, so the value of α_0 is kept fixed, where $F_0 = 0.3$ and $\omega_0 = \pi/10$, as in Fig. 1. As n grows, the frequency of the pulse grows, and spectra obtained from Eq. (1) are expected to converge to the one from Eq. (4). This is indeed the case, see Fig. 2. This holds for any polarization of the pulse. We thus conclude that the physical origin of the SEP can be sought on the basis of Eq. (4).

The third condition in (2) facilitates the analysis of Eq. (4). Under this condition, transitions caused by variations of the dressed potential can be treated in the adiabatic approximation. We are interested in transitions to the continuum. While nonadiabatic transitions between discrete states have been a subject of intensive studies since the

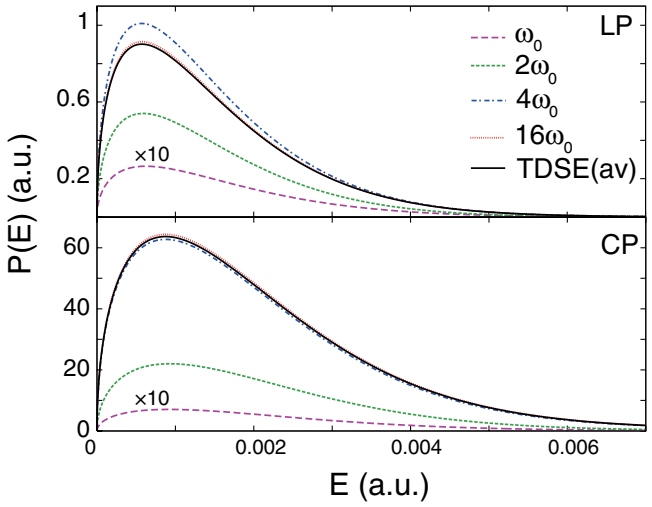

FIG. 2 (color online). Broken curves: the full TDSE results, Eq. (1), for the slow electron peak produced by pulses with $F = n^2F_0$, $\omega = n\omega_0$, and $T = 2400$, where $\omega_0 = \pi/10$, $F_0 = 0.3$, and the integer n varies from 1 to 16. The value of $\alpha_0 = 3.04$ for these pulses is kept fixed and equal to that in Fig. 1. Solid curves: the results obtained by solving the time-averaged TDSE (4). The total spectra for linear (LP) and circular (CP) polarizations are shown.

early days of quantum mechanics, see, e.g., [20] and references therein, much less is known about nonadiabatic transitions between a discrete and continuum states. The problem was raised and solved for a certain situation in an early paper by Solov'ev [21], see also his review article [22]. More recently, the theory was rederived on completely different grounds [23], which confirmed the results of [21], but also provided a way to implement them in practical calculations. We shall use the formulation of [23]. A key object in this formulation is the Siegert state (SS) defined by the Hamiltonian in Eq. (4), the one which coincides with the initial bound state of the unperturbed atom for $\alpha(t) = 0$, as a function of time t. We discuss the adiabatic approximation only for circular polarization, since the dressed potential for the present model in this case can be calculated analytically. This potential is axially symmetric about the normal to the polarization plane. To construct the SS, we use a partial-wave expansion and the outgoing-wave boundary conditions introduced in [24]; more details on this procedure will be given elsewhere. Let $k_0(t)$ and $E_0(t) = k_0^2(t)/2$ denote the momentum and energy eigenvalues for the SS. At the ends of the pulse $\alpha(\pm T/2) = 0$, hence $k_0(\pm T/2) = i\sqrt{-2E_0}$ and $E_0(\pm T/2) = E_0$. As $\alpha(t)$ grows, the dressed potential $V_0(\mathbf{r}; \alpha(t))$ becomes shallower, and at some critical point $\alpha_c = \alpha(t_c)$ the bound state disappears, i.e., $E_0(t_c) = 0$. For the present model $\alpha_c = 4.48$. For pulses shown in Figs. 1 and 2 $\max\alpha(t) = \alpha_0 = 3.04$. So the SS remains bound all the way on the real axis of time, which corresponds to the underbarrier case in the classification of [23]. Its energy $E_0(t) < 0$ goes up [its momentum $k_0(t)$ goes down along the imaginary axis in the complex k plane] on the rising part of the pulse $-T/2 < t < 0$, reaches its maximum at $t = 0$, and this evolution is repeated in the reverse order on the falling part of the pulse $0 < t < T/2$. In the adiabatic regime, a transition can efficiently occur only when the energies of the initial and final states coincide; transitions associated with a change of the energy of the system are suppressed. Thus the moment of ionization is defined by [23]

$$k_0(t) = k \rightarrow t = t(k), \tag{5}$$

where $E = k^2/2$ is the energy of the ionized electron. In the underbarrier case, this equation does not have solutions on the real t axis. A solution can be found if, reaching the maximum of $E_0(t)$ at $t = 0$, one turns to the left and goes along the imaginary axis into the upper half of the complex t plane, see Fig. 3. The value of $\alpha(t)$ is real and continues to grow along this path. The SS remains bound until the point $t_c = t(0)$, where $k_0(t_c) = 0$. This is the entrance into the continuum. The solution $t(k)$ to Eq. (5) traces a trajectory in the complex t plane passing through t_c. Only a part of this trajectory corresponding to positive values of k is needed to calculate the photoelectron spectrum in the adiabatic approximation [23]. The partial-wave spectrum is given by [23]

$$P_l(E) \approx e^{-2\mathrm{Im}S(t(k))} \left| \frac{dt(k)}{dk} \right| \left| \frac{\phi_0^{(l)}(a; t(k))}{kah_l^{(1)}(ka)} \right|^2, \tag{6}$$

where

$$S(t) = Et - \int_0^t E_0(t)dt. \tag{7}$$

Here $h_l^{(1)}(z)$ is the spherical Hankel function of the first kind and $\phi_0^{(l)}(r; t)$ are the radial functions in the partial-wave expansion of the SS eigenfunction. The radius a at which the outgoing-wave boundary condition is applied appears in Eq. (6), but the results do not depend on its value, provided that a exceeds the range of the dressed potential [23]. In Fig. 4, we compare the partial-wave photoelectron spectra obtained by solving Eq. (4) with those defined by Eq. (6) for three pulses with $T = 600$, 1200, and 2400 for the same value of α_0 as in Figs. 1 and 2.

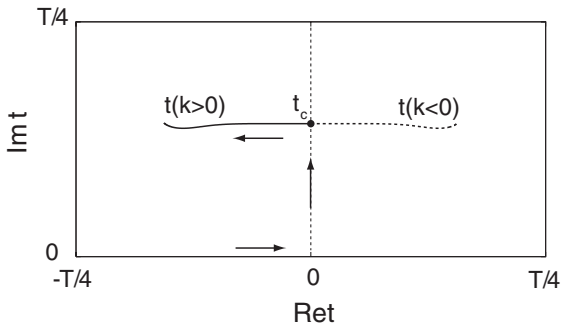

FIG. 3. An example of the trajectory traced by the solution $t(k)$ to Eq. (5) in the complex t plane. The SS is promoted to the continuum at the critical point $t_c = t(0)$.

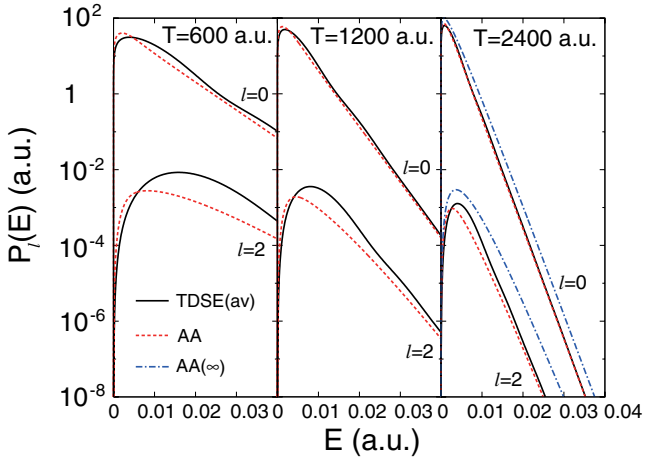

FIG. 4 (color online). The partial-wave components of the slow electron peak produced by pulses with $\alpha_0 = 3.04$, as in Figs. 1 and 2. Solid curves: the exact results obtained from the time-averaged TDSE (4). Dashed curves: the adiabatic approximation, Eq. (6). Dash-dotted curves: the limiting form of the adiabatic approximation for $T \to \infty$, Eq. (8).

The full width at half maximum for the present pulse envelope $f(\tau)$ is $T/3$, so the third condition in (2) can be specified more accurately as $|E_0|T/3 \gg 2\pi$. One can see that $T = 600$ is only the onset of the adiabatic regime. As T grows, the agreement between the exact spectra obtained from Eq. (4) and the adiabatic approximation (6) clearly improves. Thus Eq. (6) describes the SEP in the adiabatic regime. An advantage of having this approximation is that now we can extract the dependence of the SEP on the electron energy E and pulse length T analytically. In an ultimate adiabatic limit $T \to \infty$ the width of the SEP tends to zero, so all the characteristics of the SS needed to implement Eq. (6) can be substituted by their values at $t = t_c$. We thus obtain

$$P_l(E) \approx A_l T k^{2l+1} e^{-BT-2|\tau_c|TE}, \tag{8}$$

where the coefficients A_l, B, and $\tau_c = t_c/T$ depend on the atomic potential $V(r)$ and pulse envelope $f(\tau)$, but do not depend on E and T. The spectra obtained from Eq. (8) for the longest pulse with $T = 2400$ are shown in Fig. 4. Equation (8) is less accurate than Eq. (6), but is certainly correct qualitatively. One consequence of Eq. (8) is that the SEP has a very simple and typical energy dependence for the adiabatic regime [23,25]. Another consequence is that the width of the SEP and the total yield of slow electrons scale with T as T^{-1} and $T^{-1/2}e^{-BT}$, respectively. The critical moment t_c appears in Eq. (8) and hence is an observable characteristic. The main dependence on the field amplitude is hidden in the value of t_c and is not that simple to extract.

In summary, we discussed the appearance of a slow electron peak in photoelectron spectra produced by intense high-frequency laser pulses. The peak is a robust feature and exists for any polarization of the laser field. It results from promoting the atomic electron to the continuum via a nonadiabatic transition [21,23] caused by slow deformation of the dressed potential that follows a variation of the envelope of the laser pulse. This ionization mechanism should reveal itself in all spectra produced by high-frequency pulses of finite length. Being a function of the pulse envelope, the slow electron peak could serve as a measure of the pulse length or intensity.

O. I. T. thanks A. M. Popov for useful discussions and the Russian Science Support Foundation for a financial support. This work was supported by the 21st Century COE program on "Innovations in Coherent Optical Science" and by the Japan Society for the Promotion of Science (JSPS), and also in part by the PRESTO program of JST, Japan, and by a Grant-in-Aid for Scientific Research (C) from the MEXT, Japan.

[1] A. A. Sorokin *et al.*, Phys. Rev. Lett. **99**, 213002 (2007).
[2] R. Moshammer *et al.*, Phys. Rev. Lett. **98**, 203001 (2007).
[3] Y. H. Jiang *et al.*, Phys. Rev. Lett. **102**, 123002 (2009).
[4] M. Gavrila, J. Phys. B **35**, R147 (2002).
[5] A. M. Popov, O. V. Tikhonova, and E. A. Volkova, J. Phys. B **36**, R125 (2003).
[6] H. A. Kramers, *Collected Scientific Papers* (North-Holland, Amsterdam, 1956), p. 272.
[7] W. C. Henneberger, Phys. Rev. Lett. **21**, 838 (1968).
[8] M. Gavrila and J. Z. Kaminski, Phys. Rev. Lett. **52**, 613 (1984).
[9] K. Toyota, O. I. Tolstikhin, T. Morishita, and S. Watanabe, Phys. Rev. A **76**, 043418 (2007).
[10] K. Toyota, O. I. Tolstikhin, T. Morishita, and S. Watanabe, Phys. Rev. A **78**, 033432 (2008).
[11] O. I. Tolstikhin, Phys. Rev. A **77**, 032712 (2008).
[12] V. C. Reed and K. Burnett, Phys. Rev. A **43**, 6217 (1991).
[13] O. I. Tolstikhin, Phys. Rev. A **73**, 062705 (2006).
[14] O. I. Tolstikhin, Phys. Rev. A **74**, 042719 (2006).
[15] S. Yoshida *et al.*, Phys. Rev. A **60**, 1113 (1999).
[16] S. Tanabe *et al.*, Phys. Rev. A **63**, 052721 (2001).
[17] R. Santra, J. M. Shainline, and C. H. Greene, Phys. Rev. A **71**, 032703 (2005).
[18] P. Agostini *et al.*, Phys. Rev. Lett. **42**, 1127 (1979).
[19] J. H. Eberly, J. Javanaien, and K. Rzążewski, Phys. Rep. **204**, 331 (1991); R. R. Freeman and P. H. Bucksbaum, J. Phys. B **24**, 325 (1991); K. Burnett, V. C. Reed, and P. L. Knight, J. Phys. B **26**, 561 (1993).
[20] H. Nakamura, *Nonadiabatic Transition: Concepts, Basic Theories, and Applications* (World Scientific, Singapore, 2002).
[21] E. A. Solov'ev, Zh. Eksp. Teor. Fiz. **70**, 872 (1976) [Sov. Phys. JETP **43**, 453 (1976)].
[22] E. A. Solov'ev, J. Phys. B **38**, R153 (2005).
[23] O. I. Tolstikhin, Phys. Rev. A **77**, 032711 (2008).
[24] P. A. Batishchev and O. I. Tolstikhin, Phys. Rev. A **75**, 062704 (2007); (unpublished).
[25] Yu. N. Demkov and V. N. Ostrovskii, *Zero-Range Potentials and Their Applications in Atomic Physics* (Plenum Press, New York, 1988).